Mycological Progress (2023) 22:27
https://doi.org/10.1007/s11557-023-01875-8

DGfM

ORIGINAL ARTICLE

Studies on Argentine *Phylacia* species (*Hypoxylaceae*) using a polythetic taxonomic approach

Christopher Lambert[1,2,3] · Rahel Schiefelbein[1,2] · Javier A. Jaimez[4] · Marc Stadler[1,2] · Esteban B. Sir[5]

Received: 15 December 2022 / Revised: 8 February 2023 / Accepted: 9 February 2023 / Published online: 21 March 2023

Abstract

The current study is dedicated to the taxonomy of the genus *Phylacia* (*Hypoxylaceae*) in Argentina. Fieldwork in the north of the country provided several fresh collections that were studied, using a polyphasic approach. The secondary metabolite profiles of the specimens were generated by high-performance liquid chromatography hyphenated by diode array and mass spectrometry (HPLC–DAD/MS) of the stromata. This study confirmed the presence of secondary metabolites that are also found in the related genus *Daldinia*. The detection of binapththalene tetrol (BNT), daldinal B, and daldinol, which are also characteristic of certain species of *Daldinia* and *Hypoxylon*, further confirmed the chemotaxonomic affinities within the *Hypoxylaceae*. The phylogenetic affinities of several species were determined using a multi-gene genealogy based on ITS, LSU, *TUB2*, and *RPB2* sequences, confirming that *Phylacia* is most closely related to *Daldinia*, *Rhopalostroma*, and *Thamnomyces*. The new species *P. lobulata*, which features a rather unique stromatal morphology and seems to exhibit apparent host specificity for the endemic tree *Pseudobombax argentinum*, is described.

Keywords Chemotaxonomy · Phylogeny · *Sordariomycetes* · *Xylariales* · One new species

Introduction

Phylacia Lev. constitutes a small genus of the *Hypoxylaceae* (*Xylariales*), which currently includes 12 species (Wijayawardene et al. 2022), which have almost exclusively been reported from the Neotropics. The most recent overview on the taxonomy and biogeography of the genus by Medel et al. (2006) emphasized on material from Mexico. However, this paper did not evaluate type specimens of previously described taxa. Neither did Rodrigues and Samuels (1989), who were the first to describe the anamorphs. These authors classified the conidial stages of three species to be "geniculosporium-like" (sensu Petrini and Petrini 1985), but their Figs. 14 and 15 clearly show that this was a misinterpretation. The conidiogeneous cells shown do not bear any geniculate scars that result from dehiscence of conidia (cf. figure 1C in Petrini and Petrini 1985), but they should rather be classified as nodulisporium-like (sensu Petrini and Petrini 1985—cf. their fig. 1E—as well as in the anamorph classification established by Ju and Rogers 1996). For the taxonomic history of the genus, however, the paper by Rodrigues and Samuels (1989) constitutes a very valuable and complete source. Therefore, we refer to this publication for details and will here only discuss the characteristics of *Phylacia* in view of modern, polythetic concepts.

Phylacia spp. are characterized by elongated ellipsoid translucent yellow-brownish ascospores arranged in globose, evanescent asci that break up early in development and are arranged in carbonaceous, cleistothecial ascomata, which have no ostiolar canal. The asci lack an apical apparatus, and spores are not actively discharged but released after rupture

Section Editor: Marco Thines

✉ Marc Stadler
marc.stadler@helmholtz-hzi.de

Esteban B. Sir
sirestebanbenjamin@gmail.com

[1] Department Microbial Drugs, Helmholtz Centre for Infection Research GmbH, Inhoffenstraße 7, 38124 Brunswick, Germany

[2] Institute of Microbiology, Technische Universität Braunschweig, Spielmannstraße 7, 38106 Brunswick, Germany

[3] Department Cell Biology, Helmholtz Centre for Infection Research GmbH, Inhoffenstraße 7, 38124 Brunswick, Germany

[4] Facultad de Ciencias Naturales e Instituto Miguel Lillo, Universidad Nacional de Tucumán (UNT), Miguel Lillo 205, 4000 San Miguel de Tucumán, Argentina

[5] Instituto de Bioprospeccíon y Fisiología Vegetal-INBIOFIV (CONICET-UNT), San Lorenzo 1469, 4000 San Miguel de Tucumán, Tucumán, Argentina

of the ascomatal apex (Rodrigues and Samuels 1989). These characteristics are highly atypical of the *Xylariales*, but it has meanwhile been established that the characteristics of the teleomorph are not necessarily in agreement with the phylogeny of this order (Jaklitsch et al. 2016; Wendt et al. 2018; Voglmayr et al. 2022). These modern, polyphasic taxonomic studies showed that in the *Xylariales* and other groups of *Sordariomycetes*, the teleomorphic characters have subordinate importance. Anamorphic states as well as chemotaxonomic features often agree better with the molecular phylogeny than the morphology of asci and ascospores. For example, chemotaxonomic studies have revealed great similarities of *Phylacia* to the genera *Daldinia*, *Rhopalostroma*, and *Thamnomyces* (Bitzer et al. 2008; Stadler et al. 2004, 2010). The stromatal pigments of *Phylacia* closely resemble those of *Daldinia*, *Thamnomyces*, and *Rhopalostroma* (Stadler et al. 2004). A comparative study using cultures of numerous representatives of the stromatic *Xylariales* revealed a close chemotaxonomic relationship between the aforementioned genera, as well as *Entonaema* and *Ruwenzoria*, which all produced small polyketides like 1,8-naphthol, eutypinol and chromone derivatives, while *Hypoxylon* species lacked these compounds and produce mellein and isosclerone derivatives instead (Bitzer et al. 2008). This was later corroborated in a polyphasic study by Wendt et al. (2018), where *Phylacia* was placed in the family *Hypoxylaceae*, but this phylogeny did not include sequences of *Phylacia.* Other previous molecular phylogenetic studies that included a few sequences of this genus were only based on the ITS locus. In this study, we wish to fill this gap by creating additional data on *Phylacia* spp. from Argentina using morphological, chemotaxonomic, and molecular phylogenetic characters.

Experimental

General

All scientific names of fungi follow MycoBank (http://www.mycobank.org). No authorities or years of publication are given beside the taxonomic entries. Names of fungaria and culture collections are abbreviated as recommended in Index Herbariorum (http://sweetgum.nybg.org/science/ih). The chemotaxonomic studies of the stromata were carried out using the same methodology as reported recently by Cedeño-Sanchez et al. (2023).

Samples sources and morphological characterization

The fungal specimens surveyed in this study were collected in the subtropical montane forests of the Argentine Northwest. Microscopical and macroscopical morphology were examined and documented as described by Sir (2021). In addition, PVA-lactophenol was used as a mounting medium to ascertain the presence or absence of the germ slit of the ascospores.

For examination of conidiophores, HPLC profiling and sequencing, cultures of the specimens were obtained from multispore isolates according to Kuhnert et al. (2017). The morphology of cultures was studied as described by Stadler et al. (2014), using phase contrastmicroscopy and differential interference contrast under × 400–1000 optical magnification. Colors of stromatal extracts and cultures were assigned according to Rayner (1970). Cultures designated STMA are stored at interim at the HZI Braunschweig under liquid nitrogen.

DNA extraction, PCR, and molecular phylogenetics

The EZ10 Spin Column Fungal Genomic DNA Mini Preps kit (Bio Basic INC.) was used to extract genomic DNA (gDNA) following the manufacturer's protocol. For extraction, either hyphal material was removed from a YMA plate with an inoculation loop and transferred to a reaction tube with a screw cap supplied with 5–10 precellys ceramic beads (Preqlab, Germany), or material was taken from a liquid culture containing 30 mL of YM medium, which was incubated at 140 rpm and 23 °C for 2–7 days in a 150-mL Erlenmeyer flask. The samples were homogenized, and the subsequent purification steps were carried out according to the manufacturer's protocol. Samples were stored at 4 °C until further use.

Sequences of four different DNA loci (internal transcribed spacer, ITS; 28S large subunit of the ribosomal RNA, LSU; second large subunit of the nuclear RNA polymerase, *RPB2*; β-Tubulin, *TUB2*) were amplified with PCR with primers as described elsewhere (ITS: ITS1f–ITS4; Gardes and Bruns 1993 and White et al. 1990, respectively; LSU: LR0R–LR7, Vilgalys and Hester 1990; *RPB2*: fRPB25F/fRPB26F–fRPB27cR, Liu et al. 1999; *TUB2*: T1/T11–T2/T22, O'Donnell and Cigelnik 1997) and PCR programs as listed in Table 1. PCR products were purified using an EZ-10 Spin Column PCR Product Purification Kit (Bio Basic Inc.) following the manufacturers' instructions. PCR products were stored at − 20 °C until further use. Sanger DNA sequencing was performed by Microsynth Seqlab GmbH.

Sequences from a forward and a reverse read were processed using Geneious® 7.1.9 (Kearse et al. 2012). The electropherogram was checked for sequencing errors and trimmed manually. For *TUB2* and *RPB2* derived PCR sequences, sequencing was performed with four (T1, T2, T11, T22) and three different primers (fRPB25F, fRPB27cR, fRPB26F). The sequences were checked for authenticity using the NCBI (Sayers et al. 2022) BLAST® (Basic Local Alignment Search Tool; Altschul et al. 1990) program.

The MAFFT (Multiple Alignment with Fast Fourier Transform; v. 7.017) algorithm implemented in Geneious was used

Table 1 PCR programs used for the DNA loci ITS, LSU, *RPB2*, and *TUB2*

DNA Locus	Denaturation	Denaturation	Annealing	Elongation	Elongation	Cycles
ITS	94 °C (5 min)	94 °C (30 s)	52 °C (30 s)	72 °C (1:30 min)	72 °C (10 min)	35×
LSU	94 °C (5 min)	94 °C (1 min)	52 °C (1 min)	72 °C (2 min)	72 °C (10 min)	34×
RPB2	94 °C (5 min)	94 °C (30 s)	54 °C (1 min)	72 °C (2:30 min)	72 °C (10 min)	40×
TUB2	94 °C (5 min)	94 °C (30 s)	47 °C (30 s)	72 °C (3:30 min)	72 °C (10 min)	40×

to align each locus separately (Katoh and Standley 2013). The L-INS-i algorithm with a 200PAM/k = 2 scoring matrix, a gap open penalty of 1.53 and an offset value of 0.123 were used. The alignments were automatically curated with gBlocks (Castresana 2000; Castresana 2002; Talavera and Castresana 2007) as implemented in the molecular sequence data management package PhyloSuite v1.2.2 (Zhang et al. 2020).

Molecular phylogenetic trees were inferred using IQTree2 (Minh et al. 2020) following a maximum likelihood and a Bayesian (MrBayes 3.2.7a; Ronquist et al. 2012) approach. The taxon selection followed Wendt et al. (2018) with additional sequences from Sir et al. (2016). Sequence data was retrieved from GenBank (https://www.ncbi.nlm.nih.gov/gene/). An appropriate substitution model was automatically selected by ModelFinder (Kalyaanamoorthy et al. 2017), following the Bayesian information criterion (BIC) for each alignment's partition (Chernomor et al. 2016) before tree reconstruction with 1000 non-parametric bootstrap replicates (BS, Felsenstein 1985). Additionally, PartitionFinder2 (Lanfear et al. 2016) was used to determine best-fit nucleotide substitution models restricted to the ones available in MrBayes 3.2.7a following the BIC criterion. Options for the Bayesian molecular phylogenetic inference were identical to the settings used by Matio Kemkuignou et al. (2022). The topologies were compared and support values ≥ 50% (BS) or ≥ 0.95 (posterior probability, pp) assigned to the respective bipartitions. Single-gene phylogenetic inferences were carried out following the maximum likelihood criterion with 1000 bootstrap replicates to check for congruency of the resolved *Phylacia* sequences. Support values were assigned following the previously stated strategy.

Results

Molecular phylogenetic inference

Concurrently, a molecular phylogeny was inferred from a MAFFT aligned and gblocks cured multilocus dataset, which in the end consisted of 421, 1279, 957, and 1143 sites for ITS, LSU, *RPB2*, and *TUB2*, respectively (totalling a data matrix of 3800 positions). The topologies resulting from maximum likelihood and Bayesian inference strategies were compared, and support values generated from the Bayesian approach were mapped onto the maximum likelihood tree (lLn = − 38156.2560, Fig. 1). The topologies were rooted against an outgroup consisting of one representative each from the *Xylariaceae* and the *Graphostromataceae* (*Xylaria*, *Hypoxylon*, and *Graphostroma platystomum*), compared and found to be identical, with the exception of a polytomy found in the tree inferred from the Bayesian approach in the node featuring the analyzed *Phylacia* sequences (data not shown) forming a moderately bootstrap supported clade (81% BS).

Sequences of *Hypoxylon fragiforme* (the generic type) and related taxa assembled to an unresolved clade (H2, 99/1) and with sequences derived from *H. lateripigmentum*, *H. investiens*, and *H. pulicicidum* (H3, 100/1) formed a paraphyletic group. A highly supported clade (92/1) suggested relatedness of the species of H3 with *Jackrogersella* (J; 100/1) and *Annulohypoxylon* (A; 98/1), however, with *Rostrohypoxylon terebratum* (Rho) embedded into *Annulohypoxylon* with low support (within clade A; 58/0.95). Sequences derived from *Pyrenopolyporus* formed a highly supported clade (100/1) in a highly supported (88/1) sister position to the daldinoid taxa. *Daldinia* formed three lineages (D1, D2, and D3), of which the first two were resolved with high statistical support (100/1 each), while relatedness to the third clade D3 was not well supported (60/0.95). Interestingly, sequences derived from *D. korfii* clustered with sequences derived from *E. liquescens* and *Ruwenzoria pseudoannulata* (D2 + E); however, this clade received only low statistical support (55/0.96). Clade D3 clustered basally with high support (99/1) to a clade composed of the *Phylacia* sequences mentioned earlier, from which sequences derived from *Rhopalostroma* and *Thamnomyces* branched off with high and medium support, respectively (Rho, T; 99/1, 72/0.98). Sequences derived from *Hypomontagnella* (100/1; Hy) clustered with moderate support as sister group to all the former clades (62/0.99). A clade consisting of *H. fuscum* and allies (93/1; H1) appeared in a basal position (87/1) to this large cluster, to which a clade comprising *Parahypoxylon papillatum* and *Durotheca rogersii* (100/1) emerged as sister group (100/1). The resolution of the *Phylacia* clade was congruent among all single locus phylogenetic inferences (Figs. S1-S4).

Chemotaxonomy

In total, seven methanolic stromatal extracts were analyzed by HPLC–UV-Vis-ESI–MS and evaluated for the occurrence of secondary metabolites. Major constituents, characterized

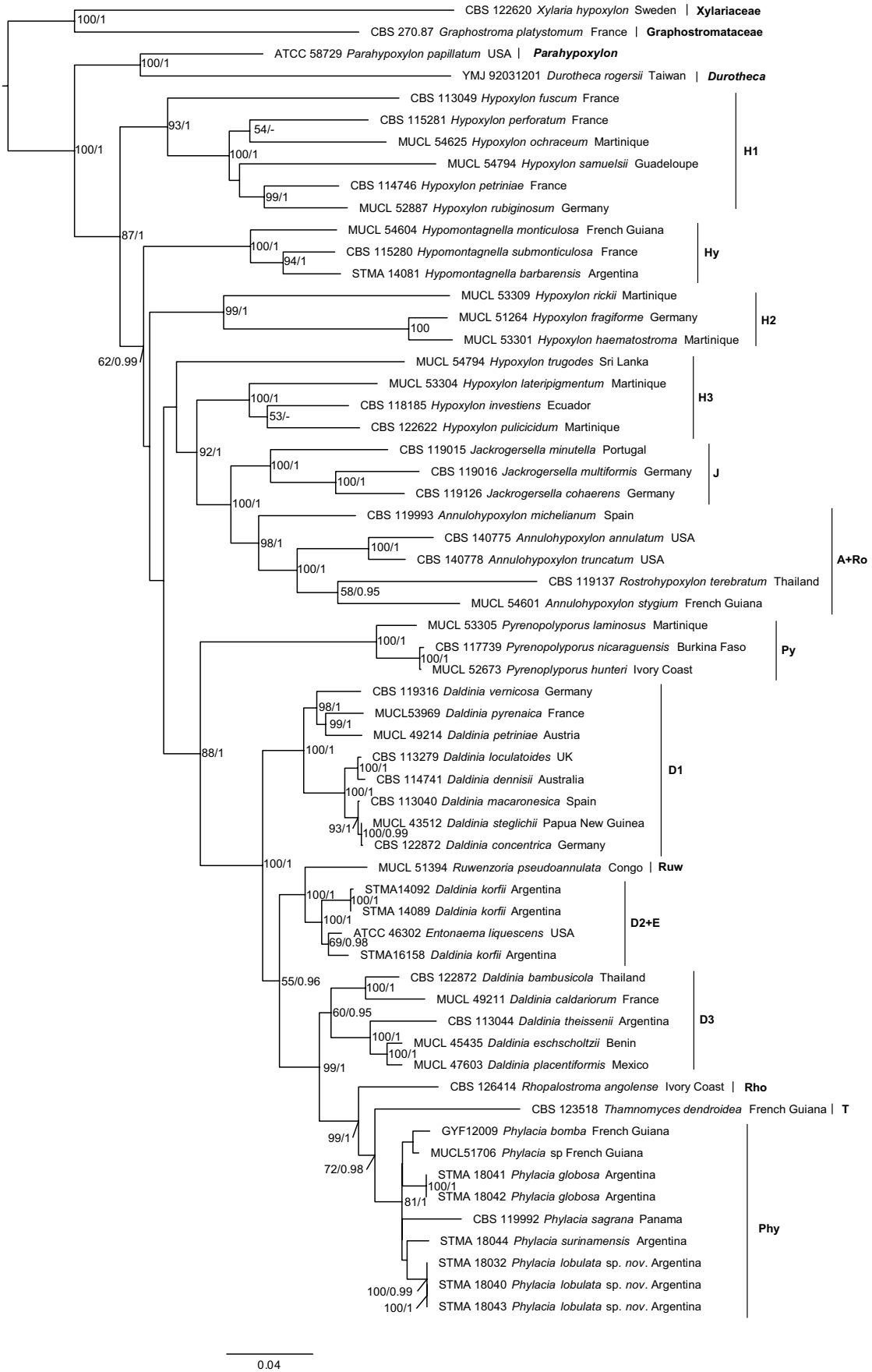
CBS 122620 Xylaria hypoxylon Sweden | Xylariaceae
CBS 270.87 Graphostroma platystomum France | Graphostromataceae
ATCC 58729 Parahypoxylon papillatum USA | Parahypoxylon
YMJ 92031201 Durotheca rogersii Taiwan | Durotheca
CBS 113049 Hypoxylon fuscum France
CBS 115281 Hypoxylon perforatum France
MUCL 54625 Hypoxylon ochraceum Martinique
MUCL 54794 Hypoxylon samuelsii Guadeloupe
CBS 114746 Hypoxylon petriniae France
MUCL 52887 Hypoxylon rubiginosum Germany
H1
MUCL 54604 Hypomontagnella monticulosa French Guiana
CBS 115280 Hypomontagnella submonticulosa France
STMA 14081 Hypomontagnella barbarensis Argentina
Hy
MUCL 53309 Hypoxylon rickii Martinique
MUCL 51264 Hypoxylon fragiforme Germany
MUCL 53301 Hypoxylon haematostroma Martinique
H2
MUCL 54794 Hypoxylon trugodes Sri Lanka
MUCL 53304 Hypoxylon lateripigmentum Martinique
CBS 118185 Hypoxylon investiens Ecuador
CBS 122622 Hypoxylon pulicicidum Martinique
H3
CBS 119015 Jackrogersella minutella Portugal
CBS 119016 Jackrogersella multiformis Germany
CBS 119126 Jackrogersella cohaerens Germany
J
CBS 119993 Annulohypoxylon michelianum Spain
CBS 140775 Annulohypoxylon annulatum USA
CBS 140778 Annulohypoxylon truncatum USA
CBS 119137 Rostrohypoxylon terebratum Thailand
MUCL 54601 Annulohypoxylon stygium French Guiana
A+Ro
MUCL 53305 Pyrenopolyporus laminosus Martinique
CBS 117739 Pyrenopolyporus nicaraguensis Burkina Faso
MUCL 52673 Pyrenoplyporus hunteri Ivory Coast
Py
CBS 119316 Daldinia vernicosa Germany
MUCL53969 Daldinia pyrenaica France
MUCL 49214 Daldinia petriniae Austria
CBS 113279 Daldinia loculatoides UK
CBS 114741 Daldinia dennisii Australia
CBS 113040 Daldinia macaronesica Spain
MUCL 43512 Daldinia steglichii Papua New Guinea
CBS 122872 Daldinia concentrica Germany
D1
MUCL 51394 Ruwenzoria pseudoannulata Congo | Ruw
STMA14092 Daldinia korfii Argentina
STMA 14089 Daldinia korfii Argentina
ATCC 46302 Entonaema liquescens USA
STMA16158 Daldinia korfii Argentina
D2+E
CBS 122872 Daldinia bambusicola Thailand
MUCL 49211 Daldinia caldariorum France
CBS 113044 Daldinia theissenii Argentina
MUCL 45435 Daldinia eschscholtzii Benin
MUCL 47603 Daldinia placentiformis Mexico
D3
CBS 126414 Rhopalostroma angolense Ivory Coast | Rho
CBS 123518 Thamnomyces dendroidea French Guiana | T
GYF12009 Phylacia bomba French Guiana
MUCL51706 Phylacia sp French Guiana
STMA 18041 Phylacia globosa Argentina
STMA 18042 Phylacia globosa Argentina
CBS 119992 Phylacia sagrana Panama
STMA 18044 Phylacia surinamensis Argentina
STMA 18032 Phylacia lobulata sp. nov. Argentina
STMA 18040 Phylacia lobulata sp. nov. Argentina
STMA 18043 Phylacia lobulata sp. nov. Argentina
Phy
0.04

◂**Fig. 1** Maximum likelihood (lLn = −38156.2560) tree inferred from ITS, LSU, *RPB2*, and *TUB2* loci of selected *Hypoxylaceae* and species of related families as outgroup. Bootstrap support values (BS) ≥ 50% and Bayesian posterior probabilities (*pp*) ≥ 0.95 are included at the respective branches

by clearly discernible peaks in the 210 nm trace, were compared with our in-house database of stromatal secondary metabolites described for different representatives of the *Hypoxylaceae* (data not shown). From a total of eleven discernible peaks relating to compounds, only compounds **2**, **6**, and **10** could be identified as daldinal B, BNT, and daldinol, respectively, with the help of standards, while **1** resembles entonalactam A. The remainder could not be safely assigned to any of the known metabolites that were previously obtained from stromata of the *Hypoxylaceae* (cf. Helaly et al. 2018). The compound detection patterns were further assigned to three chemotypes (as summarized in Fig. 3 and Table 2). It would be necessary to collect more material and do destructive preparative work and subsequent NMR spectroscopy to unambigiously identify these yet unknown compounds.

Taxonomic part

Phylacia lobulata Sir & C. Lamb., sp. nov., MycoBank N°: 846886 Figs. 1, 2, 3, 4, and 6f – j.

Etymology: The epithet *lobulata* (Latin *lobatis* = lobed) refers to stromatal morphology.

Holotype – Argentina, Jujuy province. Dept. Ledesma. Parque Nacional Calilegua, El Pedemontano trail, on dead branches of *Pseudobombax argentinum* (R.E. Fr.) A. Robyns ("soroche"), 24 May 2015, Sir and Hladki 835 (LIL 159605).

Diagnosis – Differs from all other *Phylacia* spp. by having lobed stromata and ascospores almost cylindrical with the wall slightly wider on the center of the spores.

Description – Stromata solitary to gregarious, superficial or erumpent, 9 – 22 mm long × 6 – 16 mm diam × 5 – 16 mm thick, irregularly and deeply lobed with a more or less cerebriform pattern, constricted at base, vaguely or definitely stipitate, dark brown to black, surface brown in immature stromata, dark brown with brown spots to black in mature stromata; stromal wall strongly carbonaceous, hard, disintegrating with age in an irregular area to expose the mass of ascospores; with dilute KOH-extractable pigments Greenish Olivaceous (90) after 1 min of incubation. Perithecia cylindrical-tubular 0.9 – 1.1 mm high × 0.2 – 0.4 mm diam, Asci 8 – spored, unitunicate, globose to obovoid, 16 – 29.5 µm long × 13 – 19 µm diam. Ascospores 9.2 – 11.9 (13.1) × 4.0 – 5.9 µm (*N* = 60, av. 10.9 × 4.7 µm), irregularly arranged, unicellular, pale brown to brown, strongly equilateral, ellipsoid to more or less cylindrical with rounded ends, wall thin, but slightly widening towards the center of the spore 0.5 – 0.6 µm thick, smooth, without germ slit. Conidiogeneous structure on the natural substrate as small powdery green masses at margins or over of young stromata, nodulisporium-like. Conidiophores unbranched or irregularly branched with terminal and intercalary conidiogeneous cells. Conidiophores hyaline to pale brown smooth. Conidiogeneous cells hyaline to pale brown, smooth, 8 – 32 × 1.3 – 2.4 µm, with denticulate conidial secession scars. Conidia globose, hyaline to pale brown, smooth, 2.3 – 2.8 × 1.5 – 2.5 µm.

Culture – Colonies on OA covering Petri dish in 2 weeks, at first whitish becoming Olivaceous Grey (121) velvety to felty, inconspicuously zonate with entire margins, reverse greenish black (124). Sporulation regions at the center, scattered. Conidiogeneous structure identical to that described above from the stroma.

Secondary metabolites – Stromatal extracts contain the tentatively identified entonalactam A (**1**), daldinal B (**2**), BNT (**6**) daldinol (**10**) and the unknown metabolite 8 (Fig. 2 and Table 3).

Distribution and known host – *Phylacia lobulata* is restricted to the northernmost area in the Argentine Yungas (Jujuy y Salta province). Frequently, the materials were encountered on dead branches of *Pseudobombax argentinum* (R.E. Fr.) A. Robyns, "soroche" (*Malvaceae*), (LIL 159605). Possibly, this fungus is host-specific to this plant.

Additional material studied – Argentina. Jujuy province. Dept. Ledesma. Parque Nacional Calilegua, La Lagunita trail, on dead branches of "soroche," 26 April 2014, Sir and Hladki 618 (LIL 159606), 645 (LIL 159607); on dead corticated branches, 7 June 2017, Sir 1049 (LIL 159608) 1053 (LIL 159609); same loc., El Pedemontano trail, on dead branches of dicot., 24 May 2015, Sir and Hladki 883 (LIL 159610); Guaraní trail, on dead branches of dicot. 6 June 2017, on dead branches of "sororche," Sir 1055 (LIL 159611). Salta province. Dept. Orán, road to Islas de Cañas, on dead corticated branches, 29 December 2012, Sir and Hladki 329 (LIL 159612) and 330 (LIL 159613).

Notes – This fungus is clearly a member of *Phylacia* for its cleistocarpic stomata and deliquescent asci without apical apparatus, originating from geniculate ascogeneous hyphae (Medel et al. 2006). The lobed stromata and the ascospores with thickening walls towards the spore center are the most salient discriminatory features for distinguishing it from all other known species of *Phylacia*. The latter show cylindrical, hemispherical, pulvinate, clavate, conical, pyriform, subglobose, or turbinate stroma and have ascospores with homogeneously thickened walls (Dennis 1957; Fournier and Lechat 2015; Medel et al. 2006).

Phylacia globosa Lév., Annls Sci. Nat., Bot., sér. 3 3: 61 (1845). Fig. 1, 2, and 6a–e.

For a detailed description, figure, and taxonomic notes, see Daranagama et al. (2018).

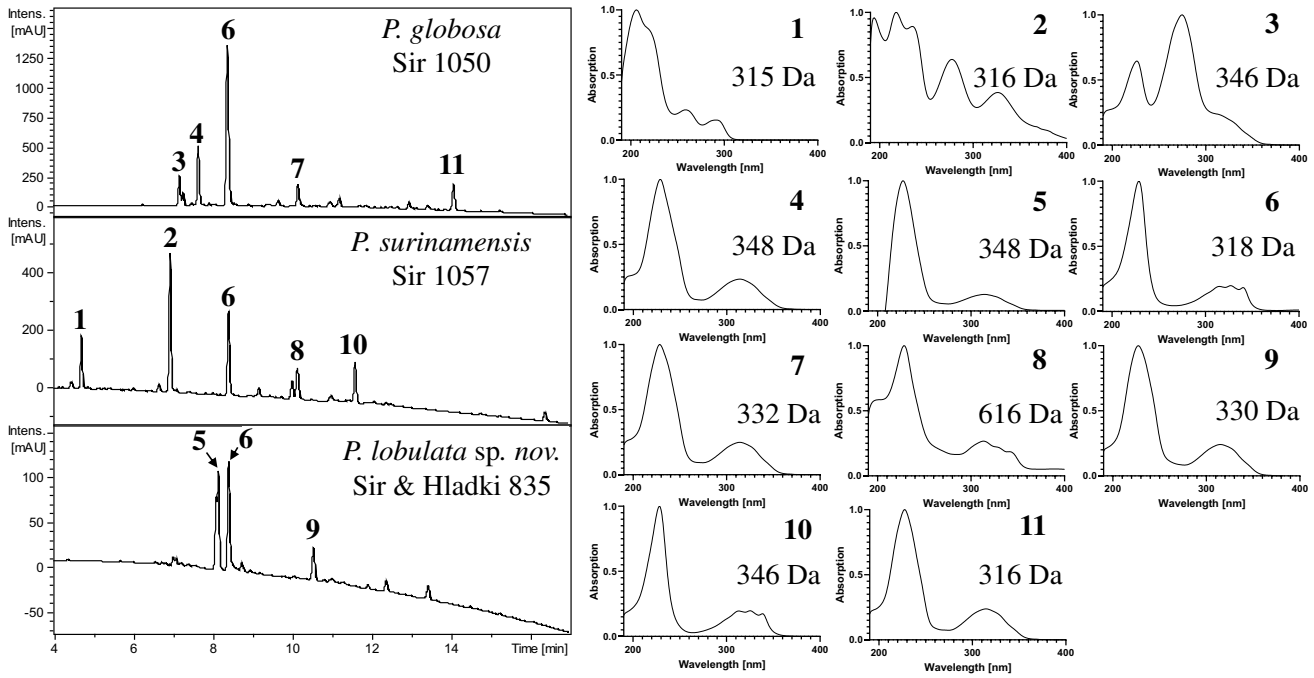

Fig. 2 HPLC chromatograms of stromatal extracts from *Phylacia* spp. collected in Las Yungas of Argentina**.** Left, representative UV chromatograms (210 nm) of methanol extracts derived from *P. globosa* (Sir 1050), *P. lobulata* sp. nov. (Sir & Hladki 835, holotype), and *P. surinamensis* (Sir 1057). Right, representative UV–Vis and mass spectra (MZ in Da). Compounds: **1** = entonalactam A; **2** = daldinal B; **3, 4, 5, 7–9, 11** = unknown; **6** = BNT; **10** = daldinol

Secondary metabolites – Stromatal extracts contain BNT (**6**) and the unknown metabolites **3**, **4**, **7**, and **11** (Fig. 2 and Table 3).

Materials studied – Argentina, Jujuy province, Dept. Ledesma. Parque Nacional Calilegua, La Junta trail, 6 June 2017, Sir 1050 (LIL 159614), 1054 (LIL159615), 1056 (LIL 159616); same loc., La Lagunita trail, 7 June 2017, Sir 1052 (LIL 159617).

Phylacia surinamensis (Berk. & M.A. Curtis) Dennis, Kew Bull. [12] (2): 325 (1957) Figs. 1, 2, 5, and 6k–o.

Description – Stromata densely caespitose, arise from the same stromal base erumpent or superficial, 2.5 – 5 mm high × 1.5 – 3.5 mm diam, more or less cylindrical to slightly clavate, constricted at center and rosette-like, with blackish carbonous surface, hard; outer crust flattened or with slightly concave apex, disintegrating with age in a defined circular area to expose the mass of ascospores, stromal wall strongly carbonaceous, externally coated by a continuous blackish crust yielding Dull Green (70) to Greenish Olivaceous (90) KOH-extractable pigments after 1 min incubation. Perithecia cylindrical-tubular 0.5 – 0.9 mm high × 0.2 – 0.3 mm diam, numerous, compact. Asci 8-spored, spherical, 14.7 – 18.8 µm diam. Ascospores (11.1) 11.5 – 13.5 (14.2) × (5.4) 5.8 – 7.5 (7.8) µm, (n = 60, av. 12.3 × 6.5 µm), irregularly arranged, unicellular, brown to pale brown ellipsoid, equilateral to slightly inequilateral with a germ slit (detectable in lactophenol) and wall thin, smooth. Conidiogenous structure not observed.

Culture – Colonies on OA covering Petri dish in 2 weeks, at first whitish becoming Olivaceous Grey (121) at the center and with entire and Pure Yellow (14) margin; velvety to felty, reverse greenish black (124). Sporulation not observed.

Secondary metabolites – Stromatal extracts contain the tentatively identified entonalactam A (**1**), daldinal B (**2**), BNT (**6**) daldinol (**10**) and the unknown metabolite 8 (Fig. 2 and Table 3).

Known distribution and host – Phylacia surinamensis is common in the urban areas of Tucuman province and is also encountered in natural reserves from Jujuy province (Argentina). The fresh stromata of this species have been found on recently dead branches and trunks of *Ceiba* sp. (*Malvaceae*). This fungus was previously recorded in Brazil (Amazonas), Guatemala, Mexico, and Surinam (Medel et al. 2006).

Materials studied – Argentina. Jujuy province. Dept. Ledesma, Parque Nacional Calilegua, road to La Lagunita trail, on dead branches of *Ceiba* sp., 11 May 2012, Sir & Hladki 042 (LIL 159618); same loc., 26 April 2014, on dead branches of *Ceiba* sp, Sir & Hladki 621 (LIL 159619); 26 May 2015, on dead branches of *Ceiba* sp., Sir & Hladki 832 (LIL 159620), 833 (LIL 159621); 6 June 2017, Guaraní trail, on dead branches of *Ceiba* sp., Sir 1051 (LIL 159622); 7 June 2017, on dead branches of *Ceiba* sp., Sir 1057 (LIL 159623). Tucuman province. Dept. Capital, Parque Avellaneda, 19 Jan 2019, on dead branches of *Ceiba* sp., Sir

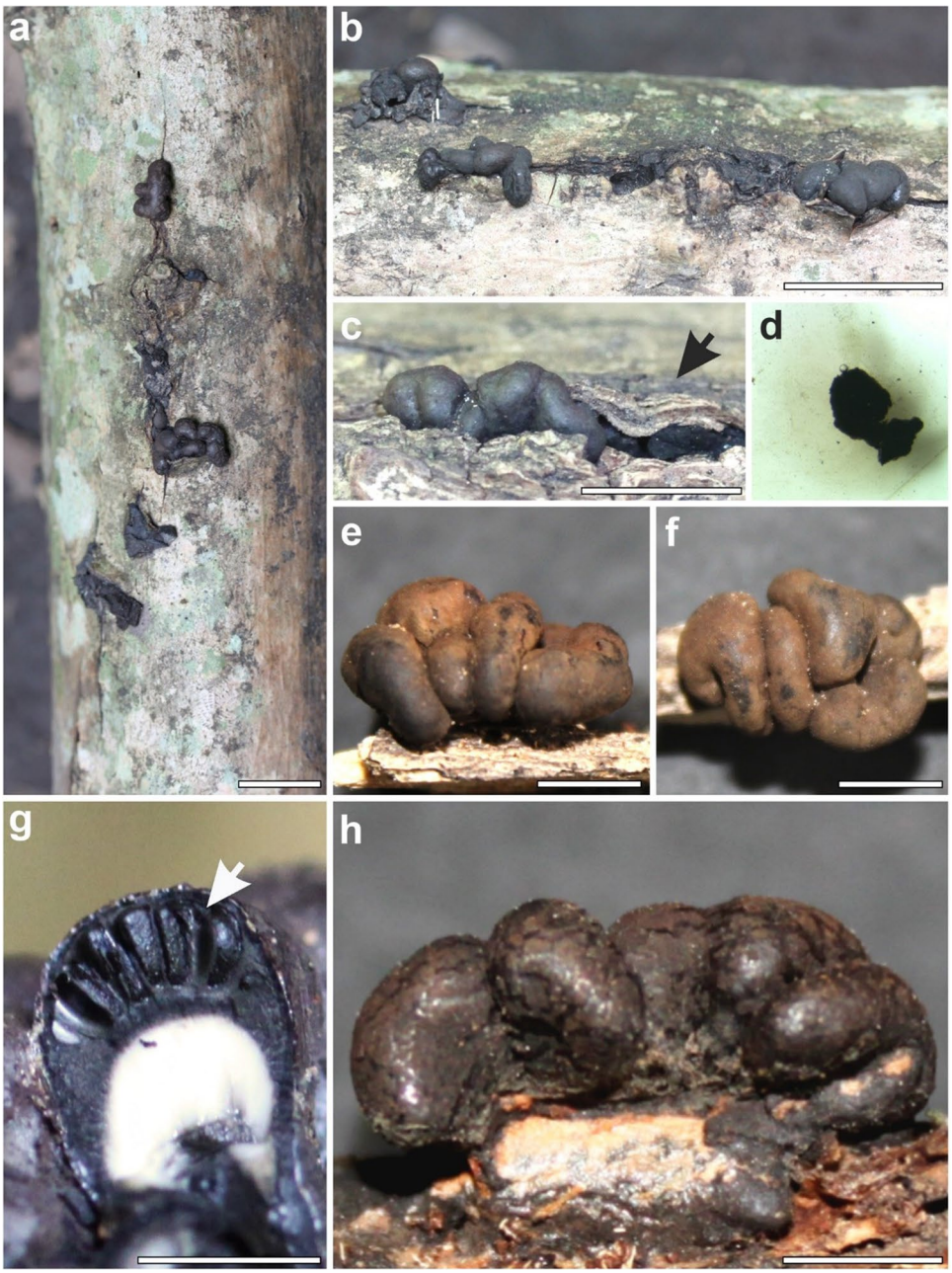

Fig. 3 Macroscopic features of *Phylacia lobulata* (holotype). **a**, **b** stromata on substrate. **c** Stromata in close-up showing the erumpent habit. **d** KOH-extractable pigments. **e** Immature stroma in lateral view. **f** Immature stroma in frontal view. **g** Stroma in vertical section showing the perithecia (arrow). **h** Mature stroma. Bars: **a**, **b** = 10 mm; **c** = 5 mm; **e**, **f** = 3 mm; **g**, **h** = 2 mm

1237 (LIL 159624); same loc., Parque 9 de Julio, 8 June 2019, dead branches of *Ceiba* sp., Sir 1238 (LIL 159625). GUATEMALA. Uaxantun, on dead *Ceiba* sp., April 1931, H.H. Bartlett 12443, det. J. H. Miller as *Camillea surinamensis* – (MICH ex LIL).

Notes – This taxon is characterized by having densely caespitose stromata and by its elliptical ascospores. Its stromata are usually cylindrical with flattened or slightly concave apex and grouped on a broad stromatic base (Dennis 1957). The Argentine materials show stromata cylindrical with slight constrictions at the center; in some cases, their shape can be almost clavate.

Phylacia cylindrica has a similar stromatal shape as *P. surinamensis*, but these species differ by the colors of KOH-extractable pigments (purple vinaceous *vs* green) and by their ascospore size (Lacerda et al. 2018). The ascospores in *Phylacia* taxa are apparently devoid of germ slits; Dennis (1957) however illustrated an ascospore with a notable germ slit for *P. surinamensis*. Lacerda et al. (2018) studied the type specimen and recognized a conspicuous germ slit in old ascospores of this species. Medel et al. (2006) also mentioned the presence of this feature for a collection of *P. sagrana* (Mont.) Mont. from Costa Rica. Fournier and Lechat (2015) also reported germ slits in ascospores of three

Table 2 List of sequences used for the molecular phylogenetic interference. Missing loci information is denoted by N/A (not available). Type status is specified by HT (holotype), ET (epitype), or PT (paratype). Sequences generated in this study are marked in bold

Species	Strain number	ITS	LSU	*RPB2*	*TUB2*	Origin and status	References
Annulohypoxylon annulatum	CBS 140775	KY610418	KY610418	KY624263	KX376353	USA (ET)	Kuhnert et al. 2014 (*TUB2*); Wendt et al. 2018 (ITS, LSU, *RPB2*)
Annulohypoxylon michelianum	CBS 119993	KX376320	KY610423	KY624234	KX271239	Spain	Kuhnert et al. 2014 (ITS, *TUB2*); Wendt et al. 2018 (LSU, *RPB2*)
Annulohypoxylon stygium	MUCL 54601	KY610409	KY610475	KY624292	KX271263	French Guiana	Wendt et al. 2018
Annulohypoxylon truncatum	CBS 140778	KY610419	KY610419	KY624277	KX376352	USA (ET)	Kuhnert et al. 2017 (*TUB2*); Wendt et al. 2018 (ITS, LSU, *RPB2*)
Daldinia bambusicola	CBS 122872	KY610385	KY610431	KY624241	AY951688	Thailand (HT)	Hsieh et al. 2005 (*TUB2*); Wendt et al. 2018 (ITS, LSU, *RPB2*)
Daldinia korfii korfii	STMA 14089	KY204020	N/A	N/A	KY204016	Argentina	Sir et al. 2016
Daldinia	STMA 14092	KY204021	N/A	N/A	KY204017	Argentina	Sir et al. 2016
Daldinia korfii	STMA 16158	KY204014	N/A	N/A	KY204020	Argentina (HT)	Sir et al. 2016
Daldinia caldariorum	MUCL 49211	AM749934	KY610433	KY624242	KC977282	France	Bitzer et al. 2008 (ITS); Kuhnert et al. 2014 (*TUB2*); Wendt et al. 2018 (LSU, *RPB2*)
Daldinia concentrica	CBS 113277	AY616683	KY610434	KY624243	KC977274	Germany	Triebel et al. 2005 (ITS); Kuhnert et al. 2014 (*TUB2*); Wendt et al. 2018 (LSU, *RPB2*)
Daldinia dennisii	CBS 114741	JX658477	KY610435	KY624244	KC977262	Australia (HT)	Stadler et al. 2014 (ITS); Kuhnert et al. 2014 (*TUB2*); Wendt et al. 2018 (LSU, *RPB2*)
Daldinia eschscholtzii	MUCL 45435	JX658484	KY610437	KY624246	KC977266	Benin	Stadler et al. 2014 (ITS); Kuhnert et al. 2014 (*TUB2*); Wendt et al. 2018 (LSU, *RPB2*)
Daldinia loculatoides	CBS 113279	MH862918.1	KY610438	KY624247	KX271246	UK (ET)	Johannesson et al. 2000 (ITS) as *D. grandis*; Wendt et al. 2018 (LSU, *RPB2*, *TUB2*)
Daldinia macaronesica	CBS 113040	KY610398	KY610477	KY624294	KX271266	Spain (PT)	Wendt et al. 2018
Daldinia petriniae	MUCL 49214	AM749937	KY610439	KY624248	KC977261	Austria (ET)	Bitzer et al. 2008 (ITS); Kuhnert et al. 2014 (*TUB2*); Wendt et al. 2018 (LSU, *RPB2*)
Daldinia placentiformis	MUCL 47603	AM749921	KY610440	KY624249	KC977278	Mexico	Bitzer et al. 2008 (ITS); Kuhnert et al. 2014 (*TUB2*); Wendt et al. 2018 (LSU, *RPB2*)
Daldinia pyrenaica	MUCL 53969	KY610413	KY610413	KY624274	KY624312	France	Wendt et al. 2018
Daldinia steglichii	MUCL 43512	KY610399	KY610479	KY624250	KX271269	Papua New Guinea (PT)	Wendt et al. 2018
Daldinia theissenii	CBS 113044	KY610388	KY610441	KY624251	KX271247	Argentina (PT)	Wendt et al. 2018
Daldinia vernicosa	CBS 119316	KY610395	KY610442	KY624252	KC977260	Germany (ET)	Kuhnert et al. 2014 (*TUB2*), Wendt et al. 2018 (ITS, LSU, *RPB2*)

Table 2 (continued)

Species	Strain number	ITS	LSU	*RPB2*	*TUB2*	Origin and status	References
Durotheca rogersii	YMJ 92031201	EF026127.1	N/A	JX507794.1	EF025612.1	Taiwan	Hsieh et al. 2010 (ITS, *TUB2*); Mirabolfathy et al. 2012 (*RPB2*)
Entonaema liquescens	ATCC 46302	KY610389	KY610443	KY624253	KX271248	USA	Wendt et al. 2018
Graphostroma platystomum	CBS 270.87	JX658535	DQ836906	KY624296	HG934108	France (HT)	Wendt et al. 2018
Hypomontagnella barbarensis	STMA 14081	MK131720	MK131718	MK135891	MK135893	Argentina (HT)	Lambert et al. 2019
Hypomontagnella monticulosa	MUCL 54604	KY610404	KY610487	KY624305	KX271273	French Guiana (ET)	Wendt et al. 2018
Hypomontagnella submonticulosa	CBS 115280	KC968923	KY610457	KY624226	KC977267	France	Kuhnert et al. 2014 (ITS, *TUB2*); Wendt et al. 2018 (LSU, *RPB2*)
Hypoxylon fragiforme	MUCL 51264	KC477229	KM186295	MK887342	KX271282	Germany (ET)	Stadler et al. 2013 (ITS); Daranagama et al. 2015 (LSU); Sir et al. 2019 (*RPB2*); Wendt et al. 2018 (*TUB2*)
Hypoxylon ochraceum	MUCL 54625	KC968937	N/A	KY624271	KC977300	Martinique (ET)	Kuhnert et al. 2014 (ITS, *TUB2*); Wendt et al. 2018 (LSU, *RPB2*)
Hypoxylon fuscum	CBS 113049	KY610401	KY610482	KY624299	KX271271	France (ET)	Wendt et al. 2018
Hypoxylon haematostroma	MUCL 53301	AM749928	KY610448	KY624258	KC977277	Martinique (ET)	Bitzer et al. 2008 (ITS); Kuhnert et al. 2014 (*TUB2*); Wendt et al. 2018 (LSU, *RPB2*)
Hypoxylon investiens	CBS 118185	KC968924	KY610451	KY624260	KC977269	Ecuador	Kuhnert et al. 2014 (ITS, *TUB2*); Wendt et al. 2018 (LSU, *RPB2*)
Hypoxylon lateripigmentum	MUCL 53304	KC968933	KY610486	KY624304	KC977290	Martinique (ET)	Kuhnert et al. 2014 (ITS, *TUB2*); Wendt et al. 2018 (LSU, *RPB2*)
Parahypoxylon papillatum	ATCC 58729	KC968919	KY610454	KY624223	KC977258	USA (HT)	Kuhnert et al. 2014 (ITS, *TUB2*); Wendt et al. 2018 (LSU, *RPB2*)
Hypoxylon perforatum	CBS 115281	KY610391	KY610455	KY624224	KX271250	France	Wendt et al. 2018
Hypoxylon petriniae	CBS 114746	KY610405	KY610491	KY624279	KX271274	France (HT)	Wendt et al. 2018
Hypoxylon pulicicidum	CBS 122622	JX183075	KY610492	KY624280	JX183072	Martinique (HT)	Bills et al. 2012 (ITS, *TUB2*); Wendt et al. 2018 (LSU, *RPB2*)
Hypoxylon rickii	MUCL 53309	KC968932	KY610416	KY624281	KC977288	Martinique (ET)	Kuhnert et al. 2014 (ITS, *TUB2*); Wendt et al. 2018 (LSU, *RPB2*)
Hypoxylon rubiginosum	MUCL 52887	KC477232	KY610469	KY624266	KY624311	Germany (ET)	Stadler et al. 2013 (ITS); Wendt et al. 2018 (LSU, *RPB2*, *TUB2)*
Hypoxylon samuelsii	MUCL 51843	KC968916	KY610466	KY624269	KC977286	Guadeloupe (ET)	Kuhnert et al. 2014 (ITS, *TUB2*); Wendt et al. 2018 (LSU, *RPB2*)
Hypoxylon trugodes	MUCL 54794	KF234422	KY610493	KY624282	KF300548	Sri Lanka (ET)	Kuhnert et al. 2014 (ITS, *TUB2*); Wendt et al. 2018 (LSU, *RPB2*)
Jackrogersella cohaerens	CBS 119126	KY610396	KY610497	KY624270	KY624314	Germany	Wendt et al. 2018

Table 2 (continued)

Species	Strain number	ITS	LSU	*RPB2*	*TUB2*	Origin and status	References
Jackrogersella minutella	CBS 119015	KY610381	KY610424	KY624235	KX271240	Portugal	Kuhnert et al. 2017 (*TUB2*), Wendt et al. 2018 (ITS, LSU, *RPB2*)
Jackrogersella multiformis	CBS 119016	KC477234	KY610473	KY624290	KX271262	Germany (ET)	Kuhnert et al. 2014 (ITS); 2016 (*TUB2*); Wendt et al. 2018 (LSU, *RPB2*)
Parahypoxylon papillatum	ATCC 58729	KC968919	KY610454	KY624223	KC977258	USA (HT)	Kuhnert et al. 2014 (ITS, *TUB2*); Wendt et al. 2018 (LSU, *RPB2*)
Phylacia bomba	GYJF12009	KC477238	N/A	N/A	N/A	French Guiana	Stadler et al. (2013)
Phylacia globosa	**STMA 18042**	**OQ437889**	**OQ437885**	**OQ453168**	**OQ453172**	**Argentina**	**This study**
Phylacia globosa	**STMA 18041**	**OQ437888**	**OQ437884**	**OQ453169**	**OQ453173**	**Argentina**	**This study**
Phylacia sagrana	CBS 119992	AM749919	N/A	N/A	N/A	Panama	Bitzer et al. 2008
***Phylacia lobulata* sp. nov.**	**STMA 18032**	**OQ437892**	**OQ437882**	**OQ453166**	**N/A**	**Argentina (HT)**	**This study**
***Phylacia lobulata* sp. nov.**	**STMA 18043**	**OQ437890**	**OQ437886**	**OQ453165**	**OQ453171**	**Argentina**	**This study**
***Phylacia lobulata* sp. nov.**	**STMA 18040**	**OQ437893**	**OQ437883**	**OQ453164**	**OQ453170**	**Argentina**	**This study**
Phylacia surinamensis	**STMA 18044**	**OQ437891**	**OQ437887**	**OQ453167**	**N/A**	**Argentina**	**This study**
Phylacia poculiformis	MUCL 51706	FN428830	N/A	N/A	N/A	French Guiana	Stadler et al. 2010
Pyrenopolyporus hunteri	MUCL 52673	KY610421	KY610472	KY624309	KU159530	Ivory Coast (ET)	Wendt et al. 2018
Pyrenopolyporus laminosus	MUCL 53305	KC968934	KY610485	KY624303	KC977292	Martinique (HT)	Kuhnert et al. 2014 (ITS, *TUB2*); Wendt et al. 2018 (LSU, *RPB2*)
Pyrenopolyporus nicaraguensis	CBS 117739	AM749922	KY610489	KY624307	KC977272	Burkina Faso	Bitzer et al. 2008 (ITS); Kuhnert et al. 2014 (*TUB2*); Wendt et al. 2018 (LSU, *RPB2*)
Rhopalostroma angolense	CBS 126414	KY610420	KY610459	KY624228	KX271277	Ivory Coast	Wendt et al. 2018
Rostrohypoxylon terebratum	CBS 119137	DQ631943	DQ840069	DQ631954	DQ840097	Thailand (HT)	Tang et al. 2007; Fournier et al. 2010
Ruwenzoria pseudoannulata	MUCL 51394	KY610406	KY610494	KY624286	KX271278	D. R. Congo (HT)	Wendt et al. 2018
Thamnomyces dendroidea	CBS 123578	FN428831	KY610467	KY624232	KY624313	French Guinea (HT)	Stadler et al. 2010 (ITS); Wendt et al. 2018 (LSU, *RPB2*, *TUB2*)
Xylaria hypoxylon	CBS 122620	KY610407	KY610495	KY624231	KX271279	Sweden (ET)	Sir et al. 2016 (*TUB2*); Wendt et al. 2018 (ITS, LSU, *RPB2*)

species: *P. bomba*, *P.* cf. *sagrana*, and *P. korfii*, when the spores were mounted in PVA-lactophenol.

The salient discriminatory features of *P. surinamensis*, *P. globosa*, and *P. lobulata* are summarized and compared in Table 4 and illustrated in Fig. 6.

Discussion

This study reports several new records of *Phylacia* collected in Argentina that were analyzed by a polyphasic approach using a multigene molecular phylogenetic inference and a

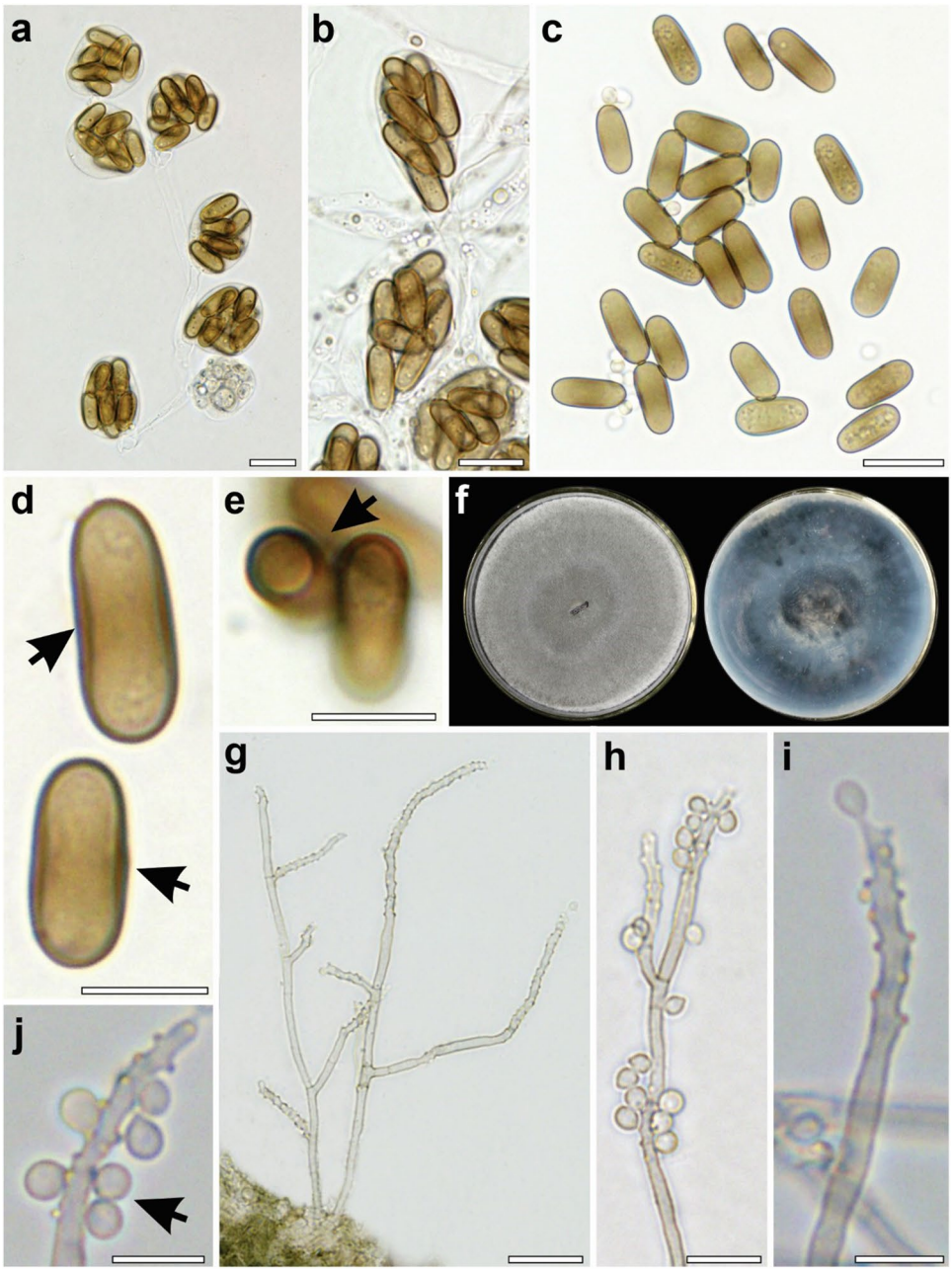

Fig. 4 Microscopic features of *Phylacia lobulata* (holotype) and culture. **a, b** Asci in 3% KOH solution. **c** Ascospores in water. **d** Ascospores in lactophenol showing wall thickening (arrow). **e** Ascospores in lactophenol seen from one end (arrow). **f** Culture on oatmeal agar after 2 weeks. **g**, **h** Conidiophores in 3% KOH solution. **i** Conidiogenous cell in 3% KOH solution. **j** Conidiogeneous cells and conidia (arrow) in 3% KOH solution. Bars: **a**, **b**, **c**, **g**, **h** = 10 µm; **d**, **e**, **i**, **j** = 5 µm

chemotaxonomic study of their stromatal constituents by HPLC–DAD-MS. The affinities of the genus to *Daldinia* and *Thamnomyces* were already described by Ju et al. (1997), which was later corroborated by a chemotaxonomic study on the type and authentic specimens by Stadler et al. (2004). In that paper, binaphthalene derivatives such as BNT, azaphilones of the daldinin type, and daldinal derivatives were reported from stromatal extracts of *P. bomba*, *P. globosa*, *P. poculiformis*, *P. sagraena*, *P. surinamensis*, and *P. turbinata.* These secondary metabolites are commonly encountered in certain species of *Daldinia (D. childiae* group; cf. Stadler et al. 2014), but also occur in the *Hypoxylon fuscum* complex (Stadler et al. 2008b; Lambert et al. 2021). This paper is thus the first to use an integrative approach to the taxonomy of the genus that relies on a significant number of freshly collected specimens.

Another chemotaxonomic study of numerous strains that now belong in the *Hypoxylaceae* included a culture of *Phylacia sagrana* (CBS 119992), which produced several small polyketides, present also in the concurrently studied cultures of *Daldinia* spp., but apparently absent in cultures of *Annulohypoxylon*, *Hypoxylon*, and other genera now classified as *Jackrogersella* or *Pyrenopolyporus* (Bitzer et al. 2008; see also Wendt et al. 2018 for the current taxonomy of these

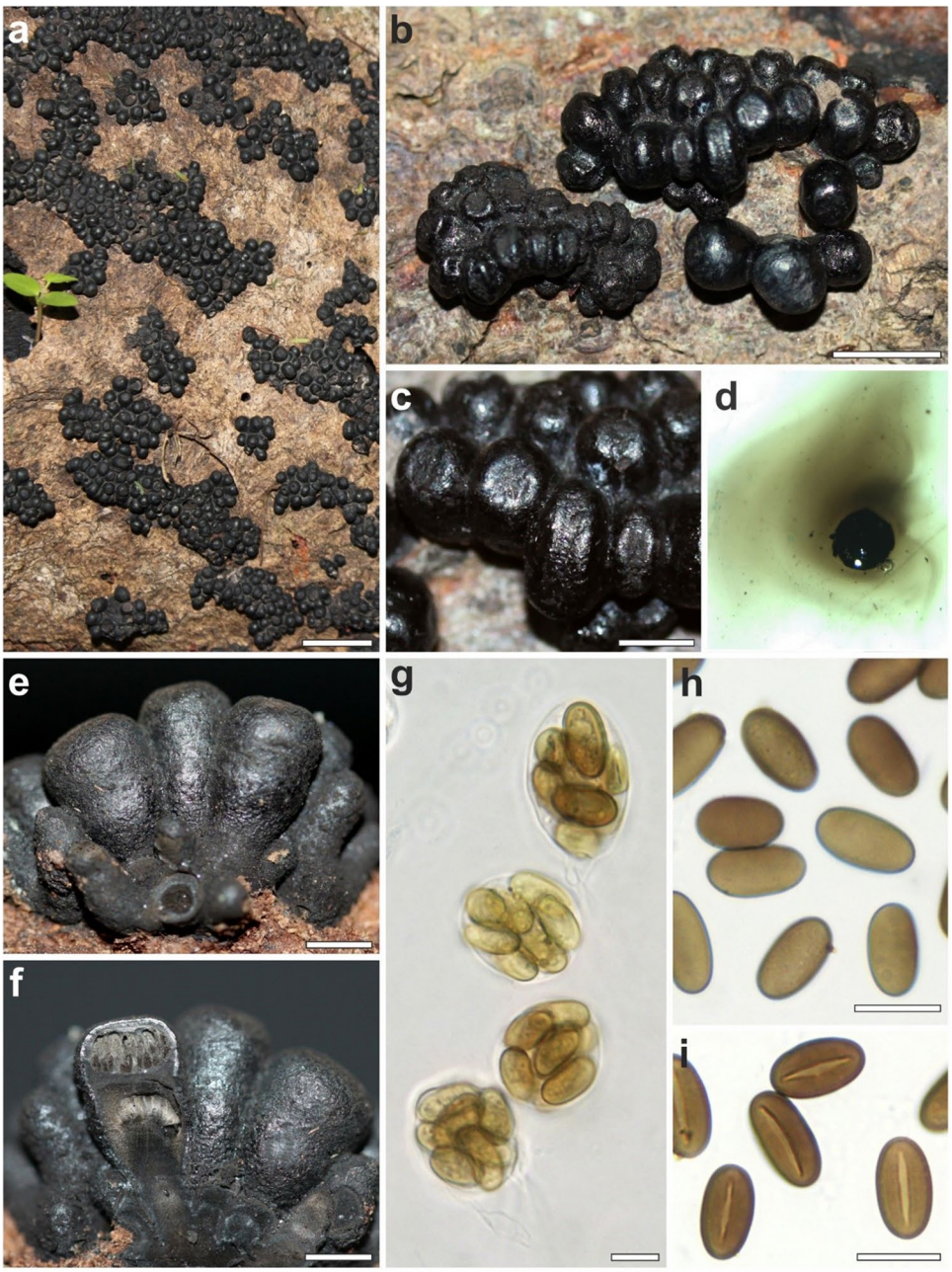

Fig. 5 *Phylacia surinamensis* (Sir 1057 - LIL 159623). **a**, **b** Stromata on substrate. **c** Detail of stroma top. **d** KOH-extractable pigments. **e** Stroma in lateral view. **f** Stroma in vertical section. **g** Asci in 3% KOH solution. **h** Ascospores in water. **i** Ascospores in PVA-lactophenol. Bars: **a** = 10 mm; **b** = 2 mm; **c**, **d**, **f** = 1 mm; **g**, **h**, **i** = 10 µm

genera and species). The secondary metabolite profile of this *Phylacia* culture was most similar to that of *D. caldariorum*, to which it also showed the closest phylogenetic relationship in an ITS-based phylogenetic tree. A similar pattern was described for a subsequent study focusing on *Thamnomyces* (Stadler et al. 2010), where an additional species of *Phylacia* (*P. poculiformis*) was included. The sequences of the two *Thamnomyces* spp. and both *Phylacia* species were shown to resolve within the same phylogenetic clade. The current study confirmed and settled the phylogenetic affinities of the genus using, for the first time for *Phylacia*, a multi-gene genealogy and resolving its placement inside the *Hypoxylaceae*. These results confirm previous studies as rDNA-derived sequence information was repeatedly shown to be of questionable utility. For the *Hypoxylaceae*, it was shown that polymorphisms of the rDNA cistron on the one hand, and high redundancies of ITS sequences across several species complexes occur on the other hand (see Stadler et al. 2020 and Maharachchikumbura et al. 2021 for an extensive discussion of this matter).

Our investigation on chemotaxonomically informative secondary metabolites in the stromatal extracts yielded compounds with five different UV–Vis spectra types. In *P. surinamensis* Sir 1056, a metabolite (**1**) occurred whose

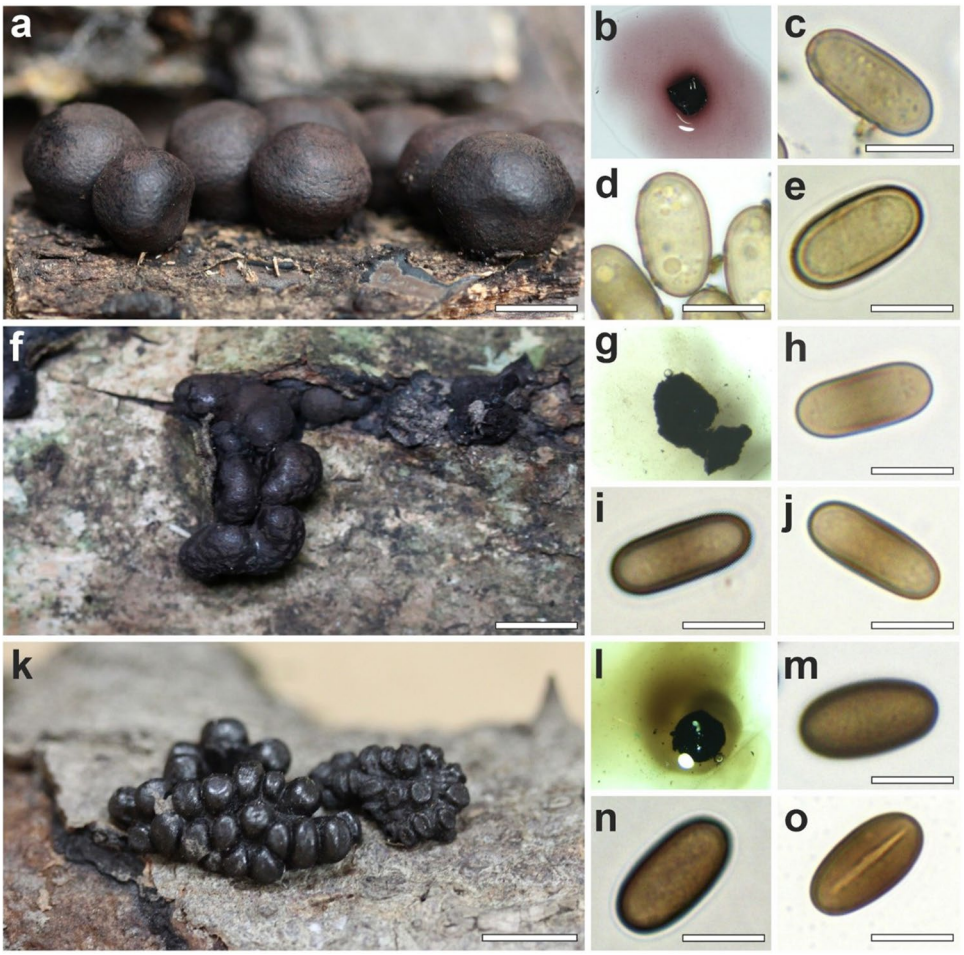

Fig. 6 *Phylacia* spp. from Las Yungas of Argentina (**a**–**e** *P. globosa* (Sir 1050 - LIL 159614), **f**–**j** *P. lobulata* (holotype), **k**–**o** *P. surinamensis* (Sir 1057 - LIL 159623) p–t). **a**, **f**, **k** Stromata on substrate. **b**, **g**, **l** KOH-extractable pigments. **c**, **h**, **m** Ascospores in water. **d**, **i**, **n** Ascospores in KOH 3% solution. **e**, **j**, **o** Ascospores in PVA-lactophenol. Bars: **a**, **f**, **k** = 10 mm; **c**, **d**, **h**, **i**, **j**, **m**, **n**, **o** = 10 µm

UV–Vis and mass spectra are reminiscent of the reported spectra for entonalactam A, isolated and reported from the stromata of an Australian fungus assigned to *Entonaema* sp. by Choomuenwai et al. (2015). However, since the authors did not specify how the fungus was identified and did not deposit a voucher, the identity of the material remains unclear. In the same specimen, three other compounds were found that were not detected in the other *Phylacia* extracts, of which one compound (**2**) resembled daldinal B (also isolated by Choomuenwai et al. 2015), while the others (**8** and **10**) showed a characteristic triple-UV maxima in the shape of a crown, indicative of naphthalene derivatives. The mass (616 Da) of **8** suggests a dimer of **6** (318 Da), but could not be assigned to a known compound, while **10** resembled daldinol. Compound **6** could be assigned to BNT and occurred in all studied specimen. Overall, the spectra of the metabolites of *P. surinamensis* shared similarities with the ones reported for the holotype by Stadler et al. (2004). The UV–Vis spectrum of compound **3** in *P. globosa* stromata was reminiscent of daldinin derivatives, like daldinin F, but was much smaller in comparison (346 versus 460 Da for daldinin F). All other compounds (**4**, **5**, **7**, **9**, and **11**) shared a similar UV–Vis pattern, which resembled that of daldinone B, but eluted either at a more hydrophilic (**4** and **5**) or more lipophilic (**7**, **9,** and **11**) mobile phase gradient, respectively. Furthermore, compounds **4**, **7,** and **11** could only be detected in *P. globosa*, while **5** and **9** only occurred in *P. lobulata.*

Table 3 Compounds observed in the stromata of *Phylacia* spp. Compounds: **1** = entonalactam A; **2** = daldinal B, **3**–**5** = unknown; **6** = BNT, **7**–**9** = unknown; **10** = daldinol; 11 = unknown

Compound	1	**2**	**3**	**4**	**5**	**6**	**7**	**8**	**9**	**10**	**11**
P. lobulata	-	-	-	-	+	+	-	-	+	-	-
P. globosa	-	-	+	+	-	+	+	-	-	-	+
P. surinamensis	+	+	-	-	-	+	-	+	-	+	-

Table 4 Distinctive characteristics of *Phylacia* spp. from Las Yungas of Argentina

Specie	Stroma shape	KOH-extractable pigments	Ascospores			Host genus
			Size (µm)	Shape	Wall (µm)	
P. globosa	Subglobose, lightly turbinate to clavate	Vinaceous purple	11.3 – 16.9 × 5.2 – 11.4	Oblong to broadly ellipsoid	0.5–1 (1.2)	Probably on *Ocotea*
P. lobulata sp. nov.	Lobed	Greenish olivaceous	9.2 – 13.1 × 4.0 – 5.9	Ellipsoid to more or less cylindrical with rounded ends	0.5 – 0.6 (spore center)	*Pseudobombax*
P. surinamensis	Cylindrical to slightly pyriform	Olivaceous	11.1 – 14.2 × 5.4 – 7.8	Oblong to broadly ellipsoidal	> 0.5	*Ceiba*

All in all, comparison with the data of the previous study by Stadler et al. (2004) was difficult because comparative data relied mostly on ancient type specimens. In some of them, artifacts, like obvious degradation products and even compounds that may represent insecticides that were eventually added to the specimens for preservation, were detected. However, results like the detection of daldinals in *P. surinamiensis* are quite significant as that compound seems to have remained stable not only in the holotype specimen of this species for 150 years (Stadler et al. 2004), but also in several ancient specimens of *Daldinia childiae* (Stadler et al. 2014).

We did not dispose of sufficient material of the valuable specimens that would have allowed for the isolation of the unknown metabolites by preparative HPLC and confirm their chemical structures by means of nuclear magnetic resonance (NMR) spectroscopy and high-resolution MS. However, we have included retention times, mass ionization patterns, and UV/Vis spectra for all the unknown metabolites in the SI (Supplementary Figs. S1–S11) in a hope that these data can aid in future attempts to accomplish such tasks.

Our study also revealed new phylogenetically relevant evidence because we have included some taxa that were not formerly characterized using the current multi-locus approach. For example, *Entonaema liquescens* formed a well-supported cluster with *D. korfii*, a taxon that had not been included in recent phylogenies. This was rather unexpected because of the strongly diverging morphology of the respective taxa. The sequenced *Entonaema liquescens* culture presumably originated from a specimen collected in Kansas by R. Lichtwardt in 1979 (Rogers 1982; Stadler et al. 2008a). To date, it is the only one available of the genus. It was deposited by Jack D. Rogers in ATCC, following the first report on the anamorph of this genus (Rogers 1982). Concerns regarding the authenticity of this *Entonaema* strain have already been raised (Wibberg et al. 2021; Kuhnert et al. 2021). It was reported that the genome of the strain showed rather high affinities to that of *D. concentrica*. However, the biosynthesis gene clusters encoding for mitorubrin type azaphilones, which are omnipresent in the stromata of *E. liquescens*, were not detected in the genome of the ATCC strain. This phenomenon needs further study and requires authentic cultures of *E. liquescens* that can be studied for comparison.

Supplementary Information The online version contains supplementary material available at https://doi.org/10.1007/s11557-023-01875-8.

Acknowledgements We thank Sebastian Pfütze for providing HPLC chromatograms of the *Phylacia* specimens. We want to express our gratitude to Anke Skiba for expert technical assistance in culture preservation. The authors express their appreciation to the authorities of Consejo Nacional de Investigaciones Científicas y Técnicas (CONICET) and the Fundación Miguel Lillo (FML) for the constant support. The Administración de Parques Nacionales of Argentina, Ministerio de Medio Ambiente of Salta Province and Dirección Provincial de Biodiversidad of Jujuy Province are kindly acknowledged for authorization of collection.

In particular, EBS is thankful to Adriana I. Hladki from FML for her invaluable support during the study of the *Hypoxylaceae* from Northwestern Argentina.

Author contribution R.S.: methodology and analysis. C.L.: supervision, methodology, analysis, and writing—original draft preparation. J.A.J.: methodology. E.B.S.: methodology and writing—original draft preparation. M.S.: analysis, resources and writing—review and editing.

Funding Open Access funding enabled and organized by Projekt DEAL. This work was funded by the DFG (Deutsche Forschungsgemeinschaft) priority program "Taxon-Omics: New Approaches for Discovering and Naming Biodiversity" (SPP 1991). We are also grateful to the LifeScience Foundation (Munich) for a PhD stipend for C.L.

The German Academic Exchange service (DAAD) and the Ministerio de Ciencia, Tecnología e Innovación, Argentina (MINCyT), are thanked for an academic exchange grant (DAAD-PPP 57052123/MINCyT DA/13/03; Project titles: Taxonomie, Phylogenie und funktionelle Biodiversität neotropischer Xylariaceae/Taxonomía, Filogenia Y Biodiversidad Funcional De Las Xylariaceae Del Neotrópico) to Fundación Lillo, University of Buenos Aires and HZI.

Data availability All additional data (except for the DNA sequence data, which are deposited in GenBank (https://www.ncbi.nlm.nih.gov/genbank/)) are available in the manuscript or the supplementary information.

Declarations

All work on biological material presented in this paper, as well as its shipment and the long-term storage of cultures, was in accordance with a material transfer agreement between HZI and Fundacion Lillo, arising from the MINCyT/DAAD-PPP project "Taxonomía, Filogenia Y Biodiversidad Funcional De Las Xylariaceae Del Neotrópico." Cultures were initially also stored at Fundación Lilo, where they did not survive. The copies that were maintained in Germany will be transferred to the culture collection of UBA (Buenos Aires) once ongoing work on the studied strains has been finished.

Ethics approval and consent to participate N/A.

Consent for publication All authors have agreed to the publication of the manuscript.

Competing interests The authors declare no competing interests.

References

Altschul SF, Gish W, Miller W, Myers EW, Lipman DJ (1990) Basic local alignment search tool. J Mol Biol 215:403–404. https://doi.org/10.1016/S0022-2836(05)80360-2

Bills GF, Gonzalez-Menendez V, Martin J et al. (2012) *Hypoxylon pulicicidum* sp. nov. (*Ascomycota*, *Xylariales*), a pantropical insecticide-producing endophyte. PLoS One 7:e46687 https://doi.org/10.1371/journal.pone.0046687

Bitzer J, Laessøe T, Fournier J et al (2008) Affinities of *Phylacia* and the daldinoid *Xylariaceae*, inferred from chemotypes of cultures and ribosomal DNA sequences. Mycol Res 112:251–270. https://doi.org/10.1016/j.mycres.2007.07.004

Castresana J (2000) Selection of conserved blocks from multiple alignments for their use in phylogenetic analysis. Mol Biol Evol 17:540–552. https://doi.org/10.1093/oxfordjournals.molbev.a026334

Castresana J (2002) Estimation of genetic distances from human and mouse introns. Genome Biol 3(research0028):1. https://doi.org/10.1186/gb-2002-3-6-research0028

Cedeño-Sanchez M, Charria-Girón E, Lambert C, Luangsa–ard JJ, Decock C, Franke R, Brönstrup M, Stadler M, (2023) Segregation of the genus *Parahypoxylon* (*Hypoxylaceae*) from *Hypoxylon* by a polyphasic taxonomic approach. MycoKeys 95:131–162. https://doi.org/10.3897/mycokeys.95.98125

Chernomor O, von Haeseler A, Monh BQ (2016) Terrace aware data structure for phylogenomic inference from supermatrices. Syst Biol 65(6):997–1008. https://doi.org/10.1093/sysbio/syw037

Choomuenwai V, Beattie KD, Healy PC, Andrews KT, Fechner N, Davis RA (2015) Entonalactams A-C: isoindolinone derivatives from an Australian rainforest fungus belonging to the genus *Entonaema*. Phytochemistry 117:10–16. https://doi.org/10.1016/j.phytochem.2015.05.018

Daranagama DA, Camporesi E, Tian Q et al (2015) *Anthostomella* is polyphyletic comprising several genera in *Xylariaceae*. Fungal Divers 73:203–238. https://doi.org/10.1007/s13225-015-0329-6

Daranagama DA, Hyde KD, Sir EB et al (2018) Towards a natural classification and backbone tree for *Graphostromataceae*, *Hypoxylaceae*, *Lopadostomataceae* and *Xylariaceae*. Fungal Divers 88:1–165. https://doi.org/10.1007/s13225-017-0388-y

Dennis RWG (1957) Further notes on tropical American *Xylariaceae*. Kew Bull 1957:297–332

Felsenstein J (1985) Confidence limits on phylogenies: an approach using the bootstrap. Evolution 39:783–791

Fournier J, Lechat C (2015) *Phylacia korfii* sp. nov., a new species of *Phylacia* (*Xylariaceae*) from French Guiana, with notes on three other *Phylacia* spp. Ascomycete.org, 7(6):315–319. https://doi.org/10.25664/art-0154

Fournier J, Stadler M, Hyde K, Duong L (2010) The new genus *Rostrohypoxylon* and two new *Annulohypoxylon* species from Northern Thailand. Fungal Divers 40:23–36. https://doi.org/10.1007/s13225-010-0026-4

Gardes M, Bruns TD (1993) ITS primers with enhanced specificity for basidiomycetes – application to the identification of mycorrhizae and rusts. Mol Ecol 2:113–118

Helaly SE, Thongbai B, Stadler M (2018) Diversity of biologically active secondary metabolites from endophytic and saprotrophic fungi of the ascomycete order *Xylariales*. Nat Prod Rep 35:992–1014. https://doi.org/10.1039/c8np00010g

Hsieh HM, Ju YM, Rogers JD (2005) Molecular phylogeny of *Hypoxylon* and closely related genera. Mycologia 97:844–865

Hsieh HM, Lin CR, Fang MJ, Rogers JD, Fournier J, Lechat C, Ju YM (2010) Phylogenetic status of *Xylaria* subgenus *Pseudoxylaria* among taxa of the subfamily Xylarioideae (*Xylariaceae*) and phylogeny of the taxa involved in the subfamily. Mol Phylogenet Evol 54:957–969. https://doi.org/10.1016/j.ympev.2009.12.015

Jaklitsch WM, Gardiennet A, Voglmayr H (2016) Resolution of morphology-based taxonomic delusions: *Acrocordiella*, *Basiseptospora*, *Blogiascospora*, *Clypeosphaeria*, *Hymenopleella*, *Lepteutypa*, *Pseudapiospora*, *Requienella*, *Seiridium* and *Strickeria*. Persoonia 37:82–105

Johannesson H, Laessøe T, Stenlid J (2000) Molecular and morphological investigation of the genus *Daldinia* in Northern Europe. Mycol Res 104:275–280. https://doi.org/10.1017/S0953756299001719

Ju YM, Rogers JD (1996) A revision of the genus *Hypoxylon*. Mycologia Memoir n° 20. APS Press, St. Paul, p 365

Ju YM, Rogers J, San Martín F (1997) A revision of the genus *Daldinia*. Mycotaxon 61:243–293

Kalyaanamoorthy S, Minh BQ, Wong TKF, von Haeseler A, Jermiin LS (2017) ModelFinder: fast model selection for accurate phylogenetic estimates. Nat Meth 14(6):587–589. https://doi.org/10.1038/nmeth.4285

Katoh K, Standley DM (2013) MAFFT multiple sequence alignment software v. 7: improvements in performance and usability. Mol Biol Evol 30(4):772–780. https://doi.org/10.1093/molbev/mst010

Kearse M, Moir R, Wilson A, Stones–Havas S, Cheung M, Sturrock S, Buxton S, Cooper A, Markowitz S, Duran C, Thierer T, Ashton B, Mentjies P, Drummond A (2012) Geneious basic: an integrated and extendable desktop software platform for the organization and analysis of sequence data. Bioinformatics (Oxford, England) 28(12):1647–1649. https://doi.org/10.1093/bioinformatics/bts199

Kuhnert E, Fournier J, Peršoh D, Luangsa–ard JJD, Stadler M (2014) New *Hypoxylon* species from Martinique and new evidence on the molecular phylogeny of *Hypoxylon* based on ITS rDNA and β-tubulin data. Fungal Divers 64:181–203.https://doi.org/10.1007/s13225-013-0264-3

Kuhnert E, Sir EB, Lambert C et al (2017) Phylogenetic and chemotaxonomic resolution of the genus *Annulohypoxylon* (*Xylariaceae*) including four new species. Fungal Diver 85:1–43. https://doi.org/10.1007/s13225-016-0377-6

Kuhnert E, Navarro-Muñoz JC, Becker K, Stadler M, Collemare J, Cox RJ (2021) Secondary metabolite biosynthetic diversity in the fungal family *Hypoxylaceae* and *Xylaria hypoxylon*. Stud Mycol 99:1–43. https://doi.org/10.1016/j.simyco.2021.100118

Lacerda LT, Bezerra JL, Pereira J (2018) *Phylacia cylindrica* sp. nov. from Brazil. Mycotaxon 133(2):243–247. https://doi.org/10.5248/133.243

Lambert C, Wendt L, Hladki AI, Stadler M, Sir EB (2019) *Hypomontagnella* (*Hypoxylaceae*): a new genus segregated from *Hypoxylon* by a polyphasic taxonomic approach. Mycol Progr 18:187–201. https://doi.org/10.1007/s11557-018-1452-z

Lambert C, Pourmoghaddam MJ, Cedeño-Sanchez M, Surup F, Khodaparast SA, Krisai-Greilhuber I, Voglmayr H, Stradal TEB, Stadler M (2021) Resolution of the *Hypoxylon fuscum* complex (*Hypoxylaceae*, *Xylariales*) and discovery and biological characterization of two of its prominent secondary metabolites. J Fungi 7:131. https://doi.org/10.3390/jof7020131

Lanfear R, Frandsen PB, Wright AM, Senfeld T, Calcott B (2016) Partition Finder 2: new methods for selecting partitioned models of evolution for molecular and morphological phylogenetic analyses. Mol Biol Evol 34:772–773. https://doi.org/10.1093/molbev/msw260

Liu Y, Whelen S, Hall BD (1999) Phylogenetic relationships among ascomycetes: evidence from an RNA polymerase II subunit. Mol Biol Evol 16:1799–1808. https://doi.org/10.1093/oxfordjournals.molbev.a026092

Maharachchikumbura SSN, Chen Y, Ariyawansa HA, Hyde KD, Haelewaters D Perera RH, Samarakoon MC, Wanasinghe DN, Bustamante DE, Liu JK, Lawrence DP, Cheewangkoon R, Stadler M (2021) Integrative approaches for species delimitation in Ascomycota. Fungal Divers 109:155–179.https://doi.org/10.1007/s13225-021-00486-6

Matio Kemkuignou B, Schweizer L, Lambert C, Anoumedem EGM, Kouam SF, Stadler M, Marin-Felix Y (2022) New polyketides from the liquid culture of *Diaporthe breyniae* sp. nov. (*Diaporthales*, *Diaporthaceae*). Mycokeys 90:85–118. https://doi.org/10.3897/mycokeys.90.82871

Medel R, Rogers JD, Guzman G (2006) *Phylacia mexicana* sp. nov. and consideration of other species with emphasis on Mexico. Mycotaxon 97:279–290

Minh BQ, Schmidt HA, Chernomor O et al (2020) IQ-TREE 2: new models and efficient methods for phylogenetic inference in the genomic era. Mol Biol Evol 37:1530–1534. https://doi.org/10.1093/molbev/msaa015

Mirabolfathy M, Ju YM, Hsieh HM, Rogers JD (2012) *Obolarina persica* sp. nov., associated with dying *Quercus* in Iran. Mycoscience 54:315–320. https://doi.org/10.1016/j.myc.2012.11.003

Petrini L, Petrini O (1985) Xylariaceous fungi as endophytes. Sydowia 38:216–234

Rayner RW (1970) A mycological colour chart. Commonwealth Mycological Institute, Kew and British Mycological Society

Rodrigues KF, Samuels GJ (1989) Studies in the genus *Phylacia* (*Xylariaceae*). Mem N Y Bot Gard 49:290–297

Ronquist F, Teslenko M, van der Mark P, Ayres DL, Darling A, Höhna S, Larget B, Liu L, Suchard MA, Huelsenbeck JP (2012) MrBayes 3.2: efficient Bayesian phylogenetic inference and model choice across a large model space. Syst Biol 61(3):539–542. https://doi.org/10.1093/sysbio/sys029

Rogers JD (1982) *Entonaema liquescens*: Description of the anamorph and thoughts on its systematic position. Mycotaxon 15:500–506

O'Donnell K, Cigelnik E (1997) Two divergent intragenomic rDNA ITS2 types within a monophyletic lineage of the fungus *Fusarium* are nonorthologous. Mol Phylogenet Evol 7:103–116. https://doi.org/10.1006/mpev.1996.0376

Sayers EW, Cavanaugh M, Clark K et al (2022) GenBank Nucl Acids Res 50:161–164. https://doi.org/10.1093/nar/gky989

Sir EB (2021) La familia *Hypoxylaceae* (*Xylariales*, *Ascomycota*) en Las Yungas del Noroeste argentino. (1ª Ed.). Fundación Hongos de Argentina para la Sustentabilidad

Sir EB, Lambert C, Wendt L et al (2016) A new species of *Daldinia* (*Xylariaceae*) from the Argentine subtropical montane forest. Mycosphere 15:1–19. https://doi.org/10.5943/mycosphere/7/9/11

Sir EB, Becker K, Lambert C, Bills GF, Kuhnert E (2019) Observations on Texas hypoxylons, including two new *Hypoxylon* species and widespread environmental isolates of the *H. croceum* complex identified by a polyphasic approach. Mycologia 111(5):832–856. https://doi.org/10.1080/00275514.2019.1637705

Stadler M, Ju YM, Rogers JD (2004) Chemotaxonomy of *Entonaema*, *Rhopalostroma* and other *Xylariaceae*. Mycol Res 108:239–256. https://doi.org/10.1017/s0953756204009347

Stadler M, Fournier J, Læssøe T, Lechat C, Tichy HV, Piepenbring M (2008a) Recognition of hypoxyloid and xylarioid *Entonaema* species from a comparison of holomorphic morphology, HPLC profiles, and ribosomal DNA sequences. Mycol Progr 7:53–73

Stadler M, Fournier J, Beltrán–Tejera E, Granmo A (2008b) The "red Hypoxylons" of the temperate and subtropical Northern Hemisphere. In "A Festschrift in honor of Professor Jack D. Rogers (Glawe DA, Ammirati JF, eds.). North American Fungi 3:73–125. https://doi.org/10.2509/naf2008.003.0075

Stadler M, Flessa F, Rambold G et al (2010) Chemotaxonomic and phylogenetic studies of *Thamnomyces* (*Xylariaceae*). Mycoscience 51:189–207. https://doi.org/10.1007/s10267-009-0028-9

Stadler M, Kuhnert E, Peršoh D, Fournier J (2013) The *Xylariaceae* as model example for a unified nomenclature following the "One Fungus-One Name" (1F1N) concept. Mycology 4:5–21. https://doi.org/10.1080/21501203.2013.782478

Stadler M, Læssøe T, Fournier J, Decock C, Schmieschek B, Tichy H-V, Peršoh D (2014) A polyphasic taxonomy of *Daldinia* (Xylariaceae). Stud Mycol 77:1–143. https://doi.org/10.3114/sim0016

Stadler M, Lambert C, Wibberg D et al (2020) Intragenomic polymorphisms in the ITS region of high-quality genomes of the *Hypoxylaceae* (*Xylariales*, *Ascomycota*). Mycol Progr 19:35–245. https://doi.org/10.1007/s11557-019-01552-9

Talavera G, Castresana J (2007) Improvement of phylogenies after removing divergent and ambiguously aligned blocks from protein sequence alignments. Syst Biol 56:564–577. https://doi.org/10.1080/10635150701472164

Tang AM, Jeewon R, Hyde KD (2007) Phylogenetic relationships of *Nemania plumbea* sp. nov. and related taxa based on ribosomal ITS and *RPB2* sequences. Mycol Res 111:392–402. https://doi.org/10.1016/j.mycres.2007.01.009

Vilgalys R, Hester M (1990) Rapid genetic identification and mapping of enzymatically amplified ribosomal DNA from several *Cryptococcus* species. J Bacteriol 172:4238–4246. https://doi.org/10.1128/jb.172.8.4238-4246.1990

Voglmayr H, Tello S, Jaklitsch WM et al (2022) About spirals and pores: *Xylariaceae* with remarkable germ loci. Persoonia 49:58–98. https://doi.org/10.3767/persoonia.2022.49.02

Wendt L, Sir EB, Kuhnert E et al (2018) Resurrection and emendation of the *Hypoxylaceae*, recognised from a multigene phylogeny of the *Xylariales*. Mycol Prog 17:115–154. https://doi.org/10.1007/s11557-017-1311-3

Wijayawardene NN, Hyde KD, Dai DQ et al (2022) Outline of fungi and fungus-like taxa – 2021. Mycosphere 13:53–453

White TJ, Bruns TD, Lee SB, Taylor JW (1990) Amplification and direct sequencing of fungal ribosomal RNA genes for phylogenetics. In: Innis MA et al. (eds) PCR protocols: a guide to methods

and -applications. Academic Press USA, 315–322. https://doi.org/10.1016/B978-0-12-372180-8.50042-1

Wibberg D, Stadler M, Lambert C et al (2021) High quality genome sequences of thirteen *Hypoxylaceae* (*Ascomycota*) strengthen the phylogenetic family backbone and enable the discovery of new taxa. Fungal Divers 106:7–28. https://doi.org/10.1007/s13225-020-00447-5

Zhang D, Gao F, Jakovlić I et al (2020) PhyloSuite: an integrated and scalable desktop platform for streamlined molecular sequence data management and evolutionary phylogenetics studies. Mol Ecol Res 20:348–355. https://doi.org/10.1111/1755-0998.13096